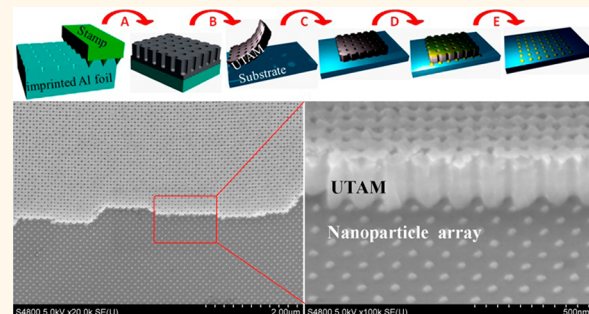


# Sub-100-nm Nanoparticle Arrays with Perfect Ordering and Tunable and Uniform Dimensions Fabricated by Combining Nanoimprinting with Ultrathin Alumina Membrane Technique

Zhibing Zhan and Yong Lei\*

Institute of Physics & Institute of Micro- and Nanotechnologies (ZIK MacroNano), Technische Universität Ilmenau, 98693 Ilmenau, Germany

**ABSTRACT** This work reports a nonlithographic nanopatterning approach to fabricate perfectly ordered nanoparticle arrays with tunable and uniform dimensions from about 30 to 80 nm and strict periods of 100 nm in a square lattice on large-area substrates by combining nanoimprinting with ultrathin alumina membrane technique. There is no requirement of any organic layer to support an ultrathin membrane in our novel route, which totally addressed the problems of nonuniform pores in prepatterned alumina templates and contamination during sample preparation, and thus is indispensable for our fabrication of ideally regular nanoparticle arrays on various kinds of substrates (such as flexible plastic). The effect of imprinted pressure on the prepatterned of Al foil was also studied in order to ensure the reusability of the precious imprinting stamps. This simple but efficient method provides a cost-effective platform for the fabrication of perfectly ordered nanostructures on substrates for various applications in nanotechnology.



**KEYWORDS:** sub-100-nm nanoparticle array · perfect ordering · uniformity · ultrathin alumina membrane · nonlithographic route

Production of perfectly ordered arrays of nanoparticles with sizes under 100 nm on large-area substrates has attracted much attention for various applications in nanotechnology, such as photoelectrical devices, data storage, and biological sensors.<sup>1–4</sup> Up to now, it is only the lithographic method that can practically produce nanoparticles with ideal regularity on relatively large areas, such as electron beam lithography, focused ion beam lithography, and nanoimprint lithography.<sup>5–8</sup> However, highly specialized lithographic facilities are complex and expensive, and tedious preparation and implementation steps (lithography and lift-off) require accuracy and time consumption.<sup>8–10</sup> As a cost-effective surface nanopatterning approach to fabricate large-scale arrays of highly defined nanostructures, anodic alumina, a typical self-ordered nanochannel material formed by anodization of Al, has been extensively explored as a template material for synthesis

of multifunctional nanostructures in a wide range of materials.<sup>8,11–14</sup> On the basis of the pioneering works by Masuda, Gosele, *et al.*, it is possible to prepare highly ordered anodic alumina *via* prepatterned an Al surface prior to the anodization process to guide the growth of the nanopores.<sup>15–21</sup> However, transferring this regular pattern on a substrate and using it as the template to fabricate ideally ordered nanostructures with tunable and uniform dimensions under 100 nm on a large area has not, to our knowledge, been previously reported, which restricted the application of alumina membranes.

By combining nanoimprinting with an ultrathin alumina membrane (UTAM) technique, we present here a nonlithographic patterning method to fabricate perfectly ordered nanoparticle arrays with tunable and uniform dimensions under 100 nm on various kinds of substrates. To our knowledge, it is challenging even for specialized lithographic approaches on this scale.<sup>22,23</sup> In our

\* Address correspondence to [yong.lei@tu-ilmenau.de](mailto:yong.lei@tu-ilmenau.de).

Received for review February 5, 2014 and accepted March 10, 2014.

Published online March 10, 2014  
10.1021/nn500713h

© 2014 American Chemical Society

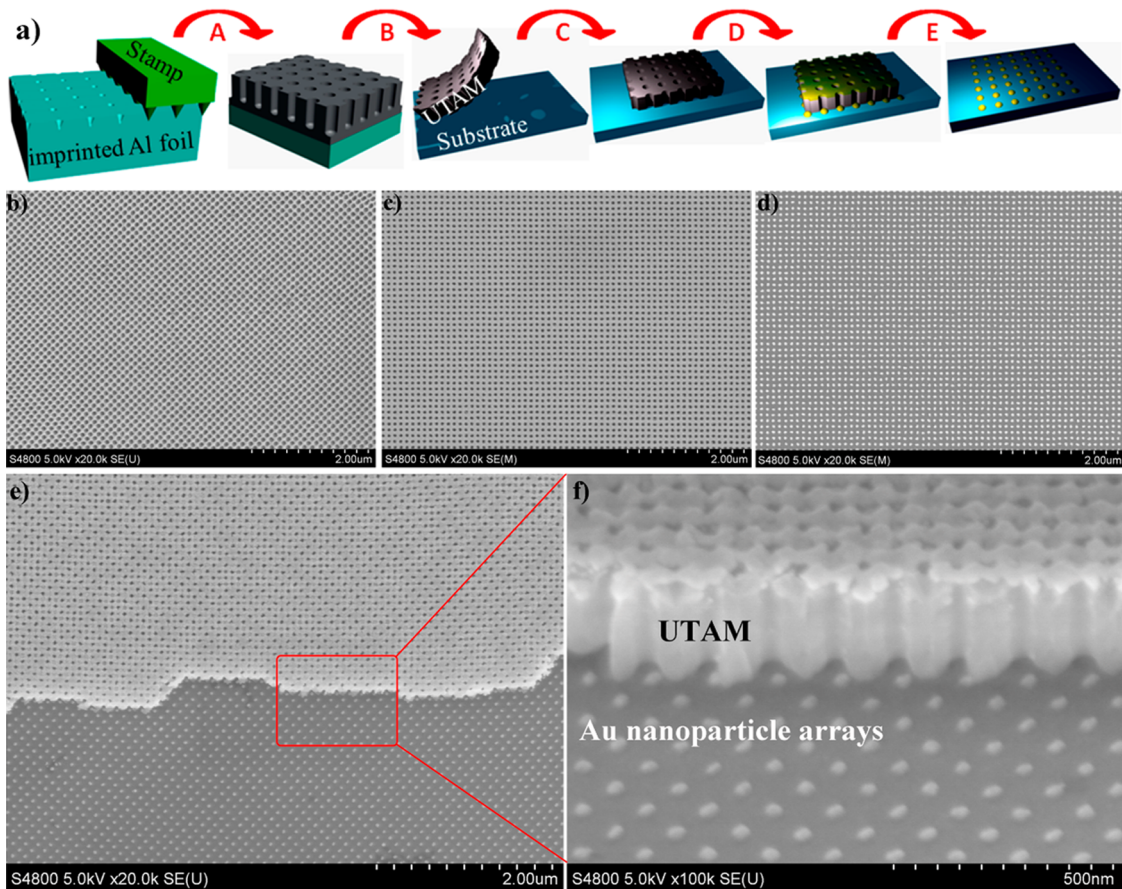


**Figure 1.** (a) Schematic outline of the fabrication processes for highly ordered nanoparticle arrays by combining nanoimprinting with UTAM technique (processes A to E are anodization of prepatterned Al foil, removal of backside Al and barrier layer and pore-widening, mounting the UTAM on the substrate, deposition of materials, and removal of UTAM, respectively). (b–f) SEM images: (b) before and (c) after deposition of Au on the UTAM, (d) Au nanoparticle arrays after totally removing the UTAM, (e and f) the intentionally remaining part of the UTAM. Image (f) is the tilted (45°) SEM of the red rectangle area in (e).

novel approach, UTAM was intactly transferred, for the first time, in different solutions without the support of any organic layer such as PMMA (poly(methyl methacrylate)), which is essential for the fabrication of ideally regular nanoparticle arrays because it thoroughly solved the problems of nonuniform dimension and contamination resulting from the use of an organic layer. Due to the reuse of imprinting stamps and no need for lithographic processes and clean-room facilities, this method offers attractive advantages, such as high throughput, cost-effectiveness, flexibility in controlling nanoparticle dimension and spacing parameters, materials and substrate universality, and massively parallel production, which may overcome problems of low throughput and high cost in conventional nanolithographic techniques<sup>8,15</sup> and offer an economical alternative to fabricate various ordered nanostructures for future nanodevices.

## RESULTS AND DISCUSSION

Highly ordered UTAMs were prepared by anodization of Al foil imprinted by a commercially purchased SiC stamp with perfect arrays of pyramid tips in a square lattice with distance periods of 100 nm. The

imprinting process generated an array of highly ordered hollows on the surface of Al foil, which replicated the negative of the rounded elevations of the imprinting stamp. Under suitable anodization voltage, each of the shallow indentations created by the imprinting process serves as a nucleation site for the development of a pore in the early stage of anodization and results in the eventual growth of a UTAM with highly ordered pore channels.<sup>15,16,18</sup> Figure 1a outlines the main fabrication processes for highly ordered nanoparticle arrays. Our brief processes include imprinting and anodization of Al foil, transferring and mounting of the UTAM, deposition of materials, and removal of the UTAM. All of those fabrication procedures were carried out in a routine laboratory rather than a clean-room. Detailed processes are described in the Experimental Section. Different from previous UTAM methods using normal two-step anodization alumina as a template,<sup>8,20,24–26</sup> there is no need for a PMMA layer to support our ideally regular UTAMs in the transfer process, which is indispensable for our fabrication of nanoparticle arrays with uniform size and perfect ordering. We will discuss this process in detail later. Figure 1b and c are top-view SEM images of a UTAM mounted on indium tin oxide (ITO)

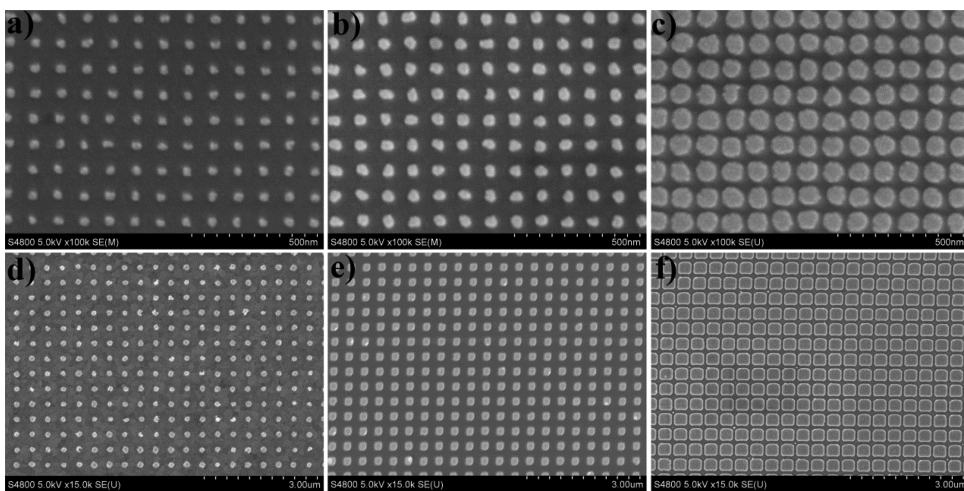


**Figure 2.** Top-view SEM images of Au nanoparticle arrays with different dimensions and periods of about (a) 30 and 100 nm, (b) 55 and 100 nm, (c) 80 and 100 nm, (d) 100 and 400 nm, (e) 200 and 400 nm, and (f) 380 and 400 nm. The corresponding durations of barrier layer removal and the pore-widening process are (a) 40, (b) 50, (c) 65, (d) 90, (e) 105, and (f) 125 min in  $H_3PO_4$  solution (5 wt %) at 30 °C.

glass before and after depositing Au. As can be seen from these images, the transferred UTAM has a perfectly ordered arrangement of nanopores in a square lattice, which has no defects in a very large area. Using this UTAM as a template, the prepared Au nanoparticles are uniform and monodispersed, and few defects were observed, as shown in Figure 1d. More large-area SEM images of a perfect UTAM and nanoparticle array are shown in Figure S1 (Supporting Information). In the top-view and tilted (45°) SEM images of Figure 1e and f, parts of the UTAM are retained intentionally, which illuminates that Au nanoparticles completely inherit the regularity of the UTAM template. This result demonstrated that our novel method can transfer the regular UTAM pattern on substrates and then fabricate perfectly ordered nanoparticles using this pattern as a template.

The dimensions of nanoparticles are determined by the size of the nanopores in templates, which can easily be controlled by the duration of the pore-widening process. As shown in Figure 2a to c, the dimensions of Au nanoparticles with periods of 100 nm can be tuned in a large range from about 30 to 80 nm just by prolonging the time of the pore-widening process. To our knowledge, fabricating and tailoring nanostructures in this range is quite challenging even for conventional lithographic approaches.<sup>22,23</sup> Furthermore, the nanoparticles distance can be adjusted by changing the periods of the imprinting stamp and choosing according anodization voltages.<sup>3,18</sup> As shown in Figure 2d to f, Au nanoparticles with periods of 400 nm were successfully fabricated *via* choosing a UTAM imprinted by a Ni stamp with periods of 400 nm and anodized under a voltage of 160 V, and the sizes of these nanoparticles can further be adjusted by a pore-widening process from about 100 to 380 nm. This kind of UTAM and Au nanoparticles prepared *via* previous methods and our new technique are shown in Figures S2 and S3.

Our approach exhibited an excellent ability to control the size, uniformity, and ordering of nanoparticles on substrates, which has important applications in the fields of size-dependent properties of nanostructures, such as surface plasmon resonance (SPR), surface-enhanced Raman spectroscopy, and photovoltaic devices or photocatalysts improved by plasmonics.<sup>9,27,28</sup>

In order to ensure the reusability of the precious imprinting stamps, it is significant to find a suitable imprinting pressure for the prepatternning of Al foil. The effect of prepatternning can be elucidated by comparing the boundary areas of a UTAM fabricated under different imprinting pressures, as shown in Figure 3. It is obvious that the porous structures produced from the nonimprinted Al area look amorphous without any ordering in terms of pore sizes, shapes, and arrangement. On the contrary, perfectly ordered porous structures can be obtained from the imprinted Al area. When the Al foil was imprinted under a pressure of 2.0 MP, only about a 1.0  $\mu$ m area near the boundary of the imprinting stamps was prepatternned successfully, as shown in Figure 3a. When the imprinted pressure increased to 4.0 MP, the prepatternned area enlarged remarkably (Figure 3b). An imprinting pressure of 6.0 MP is totally feasible for the prepatternning process, which can be confirmed in Figure 3c. Reasons for this relative low pressure is that Al foil is soft, and very shallow imprinted indentations (only 1.5 nm) can effectively guide the growth of the anodized nanopores.<sup>29</sup> This prepatternned effect for prepared nanoparticle arrays is exhibited clearly after partially removing the UTAM, as shown in Figure 3d.

As shown in Figure 4, a UTAM was intactly transferred in different solutions without the support of an organic compound layer such as PMMA due to its softness and ductility, which is crucial for our fabrication of nanostructures with perfect ordering and

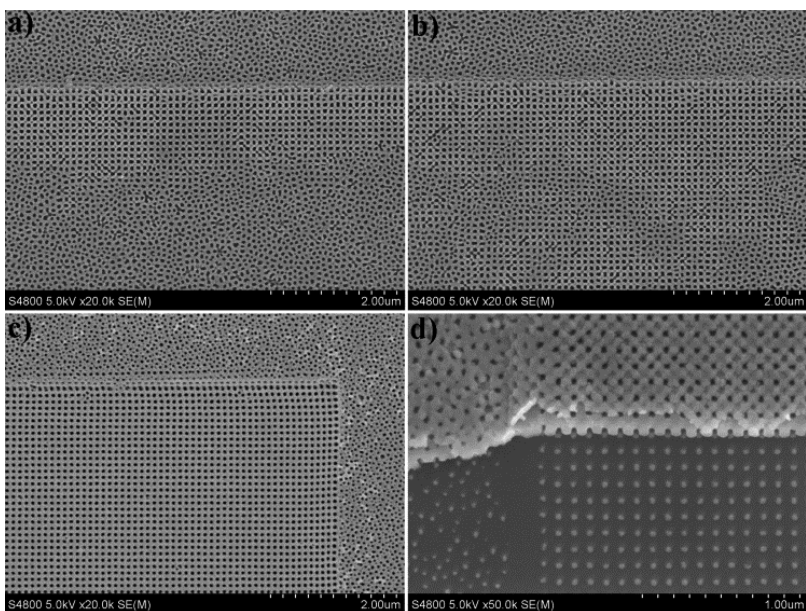


Figure 3. Top-view SEM images of a UTAM imprinted under a pressure of (a) 2.0, (b) 4.0, (c) 6.0, and (d) 6.0 MP and partly removing the UTAM.

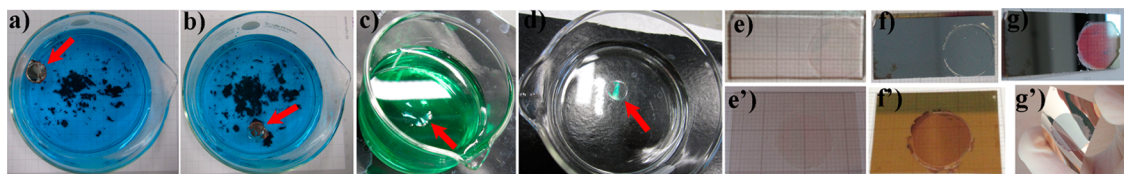
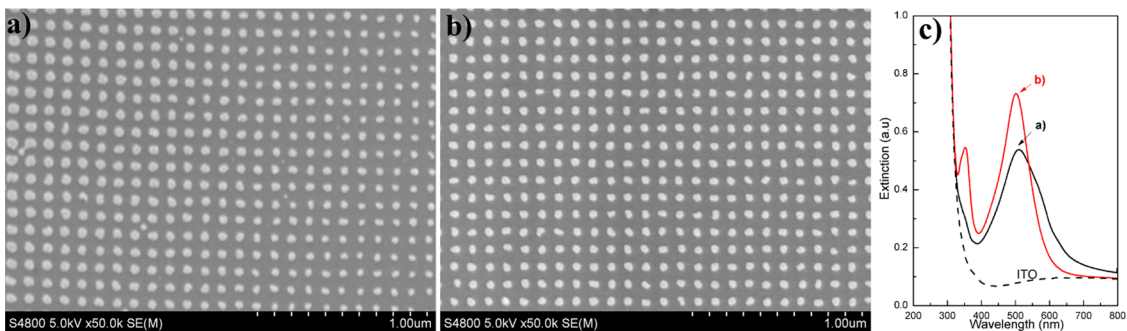


Figure 4. Photographs of the process to prepare a UTAM (indicated by red arrows) without an organic compound as supporting layer (a–d), and fabrication of a Ag nanoparticle array on an ITO-coated glass substrate (e–g) and a Au nanoparticle array on an ITO-coated polyethylene terephthalate (PET) substrate (e'–g'). The Al layer on the backside of the UTAM was rudimentarily removed in a saturated  $\text{CuCl}_2$  solution (in images (a) and (b), the brown precipitate is copper) in order to protect the UTAM; then it was further removed in mixture solutions of  $\text{CuCl}_2$  (85 wt %) and  $\text{HCl}$  (15 wt %) for 10 min, shown in (c), because this mixture solution can react slowly with UTAMs, whose reaction to backside Al is much faster than saturated  $\text{CuCl}_2$ . With the aid of a plastic strainer, the cleaned UTAM was intactly transferred to  $\text{H}_3\text{PO}_4$  solution (5 wt %) at 30 °C in order to remove the barrier layer and widen the size of the pores, as shown in (d). Images (e) and (e') illuminate that UTAMs could be ideally mounted on ITO-coated glass and PET without cracking and folding of the membranes. Images (f) and (f') show the above samples after depositing Ag and Au. Images (g) and (g') are those samples after removal of UTAMs, in which samples show a unique color due to their SPR property (red for Ag and light green for Au).

uniform size. As we know, an alumina membrane must be transferred in different liquids such as  $\text{CuCl}_2$  and  $\text{H}_3\text{PO}_4$  solutions and DI water, in order to remove the backside of Al and the barrier layer, as well as to clean the template. Generally, a layer of PMMA was coated on the UTAM to support it before removing its backside of Al (see the inset image of Figure S2a). This PMMA layer will attach to the UTAM all through the process of backside Al removal, barrier layer etching, and pore-widening until the PMMA/UTAM layer is mounted on the substrate; then the PMMA will finally be removed by organic solutions such as acetone or chloroform.<sup>8,20,24–26</sup> In actual experiments, it is difficult to ensure that the PMMA layer and the UTAM are well-attached at every point, as shown in the inset image of Figure S2a. In the process of barrier layer etching and pore-widening, the  $\text{H}_3\text{PO}_4$  solution can etch the UTAM only from the side without the PMMA layer for the areas with good attachment, but the regions without good attachment will be

etched from both sides. Therefore, the attachment between the PMMA layer and the UTAM will effect the results of pore-widening and cause a nonuniform size of the nanopores in the membrane and then the nanoparticles. As shown in Figures 5a, S2a, and S3a, this nonuniform effect is very obvious and proportional to the duration of the pore-widening process. In fact, for imprinted UTAMs, it is difficult to fabricate nanoparticle arrays with perfect ordering and uniform dimensions with the previous method of using PMMA as the supporting layer, although it seems to be no problem for the UTAM method using normal two-step anodization alumina as a template.<sup>8,20,24–26</sup> Generally, the dimensions of these nanoparticles varied gradually just in several micrometer areas, which can be confirmed clearly in Figures 5a and S3a. However, our technique presented here fully addresses this problem. There is no need for a PMMA layer to support the UTAM in our fabrication route. Therefore, the nanopores in UTAM will be etched



**Figure 5.** Top-view SEM images of Ag nanoparticles fabricated on ITO glass using a UTAM template prepared (a) with and (b) without PMMA as the supporting layer. (c) UV-vis extinction spectra of ITO glass and samples shown in (a) and (b) (the strong absorptions below a wavelength of 320 nm in both spectra are associated with the optical band gap of ITO glass).

uniformly, which is indispensable for our fabrication of nanostructures with perfect ordering and uniform size.

The uniformity of nanoparticles on much larger areas ( $\text{mm}^2$  or  $\text{cm}^2$ ) can be characterized by their SPR property, because the SPR peak is very sensitive to the parameters of nanostructures including dimension, shape, and distribution, which have been used to monitor and control nanoparticles during chemical synthesis in solution.<sup>9,30–32</sup> As can be seen from Figure 5c, Ag nanoparticles shown in Figure 5b exhibited a much narrower and sharper dipole mode of the SPR peak (at  $\sim 500$  nm) and an obvious multipole mode (at  $\sim 350$  nm) compared with those shown in Figure 5a. Because nanoparticles fabricated by this novel method have almost identical shape, size scale, distance, and surrounding conditions, their SPR peak focused consequently on the same position. On the contrary, nonuniform nanoparticles fabricated using PMMA as the supporting layer (Figure 5a) have a broad SPR distribution, and their multipole mode (which is more sensitive to the size distribution of nanoparticles than the dipole mode<sup>32</sup>) is even harder to detect, as shown in Figure 5c. Because a narrow ensemble plasmon line width is desirable for most plasmonic applications such as sensors, the enhancement of nonlinear optical effects, light guiding, labeling, or tissue targeting, the excellent controllability of nanoparticles in our method will provide guidance for future designs of plasmonic metallic nanostructures, which is significant for the application of SPR effects.<sup>33–35</sup>

Except for the nonuniformity problem, the previous method of using PMMA as the supporting layer will result in another problem, contamination, because of the final removal of the PMMA layer by organic solutions.

Our fabrication process presented here also thoroughly solved this contamination problem. Therefore, we can fabricate nanoparticles on a wider range of materials as substrates, such as flexible ITO-coated PET, as shown in Figure 4g'. Fabrication of nanostructures on flexible plastic substrates has broad applications in the field of solar cells and OLEDs (organic light-emitting diodes),<sup>36</sup> but it is inaccessible for the previous UTAM method due to the reaction between substrates and organic solutions such as acetone or chloroform. In addition, our method is totally nontoxic, more simple, and time-saving, due to omitting the process of PMMA coating, heating, and removal.

## CONCLUSION

In summary, nanoparticles with perfect ordering and tunable and uniform dimensions under 100 nm were fabricated on large-area substrates by combining nanoimprinting with the UTAM technique. Due to omitting the process of organic layer coating, heating, and removal, this approach is environmentally friendly, more simple, and time-saving and can be used to fabricate nanoparticles on any kind of substrate (such as flexible plastic). More importantly, this method also thoroughly solved the problems of nonuniform size and contamination resulting from the use of an organic layer. In addition, the effect of imprinting pressure on the prepatterned of Al foil was studied in order to ensure the reusability of the precious imprinting stamps. This nonlithographic route is a breakthrough for the broad research field of surface nanopatterning and nanostructuring, as well as related devices, and provides a cost-effective platform for the fabrication of perfectly ordered nanostructures on substrates for various nanodevices.

## EXPERIMENTAL SECTION

High-purity (99.99%) aluminum foil with a thickness of about 0.2 mm was degreased in acetone and annealed at 400 °C for 4 h under vacuum conditions to remove mechanical stresses. Then it was electrochemically polished in a 1:7 solution of perchloric acid and ethanol. The SiC imprint stamp was placed on electro-polished Al foil, and pressing was carried out using an oil press

under a pressure of about 6.0 (also 2.0 or 4.0) MP for 3 min. In order to protect the precious imprinting stamps, the pressure should be increased slowly. To ensure the effect of imprinting, the surface of the Al foil should be kept parallel to the SiC stamp during this process. After that, the SiC imprint stamps can be detached carefully from the patterned Al foil and reused. This imprinting process generated an array of highly ordered hollows

on the surface of the Al foil, which replicated the negative of the rounded protrusions of the imprint stamp. After nanoindentation, anodization was conducted under a constant voltage of 40 V in 0.3 M oxalic acid at 15 °C. This anodization voltage was chosen to satisfy the distance periods in imprint stamps due to the linear relationship between interpore distance (100 nm) and anodization potential (2.5 nm V<sup>-1</sup>). Each of the shallow indentations created by imprinting serves as a nucleation site for the development of a pore in the early stages of anodization and results in the eventual growth of highly ordered pore channels. The anodization was performed for 3 min. After anodization, the Al layer on the backside of the UTAM was rudimentarily removed in a saturated CuCl<sub>2</sub> solution and further removed in mixture solutions of saturated CuCl<sub>2</sub> (85 wt %) and HCl (15 wt %) with a concentration of 30% for 10 min. With the aid of a plastic strainer, the UTAM was transferred to a H<sub>3</sub>PO<sub>4</sub> solution (5 wt %) at 30 °C in order to remove the barrier layer and widen the size of the pores. The time for the barrier layer removal and pore-widening process depends on the desired sizes of pores in the UTAM. Then the UTAM with uniform opened pores was transferred into DI water from H<sub>3</sub>PO<sub>4</sub> solution with a plastic strainer, and the clean UTAM was mounted carefully on the substrates (including Si, ITO-coated glass, or PET) in DI water. Before this process, it is very important that the surface of the substrates is degreased and thoroughly cleaned (oxygen plasma cleaning is much better) in order to improve the attachment between UTAMs and the substrates. The mounting process can be found in ref 20 (Figure S2b). Finally, those substrates mounted with a UTAM were taken out and dried, and Au (or Ag) nanoparticles were deposited into highly ordered nanopores of the UTAM by the electron beam evaporation method (Kurt J. Lesker). During the deposition process, substrates were kept in rotation at 20 rounds per min. Then the UTAM was peeled off by Scotch tape, leaving a perfectly ordered nanoparticle array on the surface of the substrate. For the UTAM imprinted by a Ni stamp with periods of 400 nm, the anodization process was carried out in 0.4 M H<sub>3</sub>PO<sub>4</sub> acid at 160 V for 8 min. The structures of the nanoparticle array were observed by SEM (Hitachi S4800). Extinction spectra were measured by a UV-vis-NIR spectrophotometer (Cary 5000).

**Conflict of Interest:** The authors declare no competing financial interest.

**Acknowledgment.** This work was supported by a European Research Council Grant (Three-D Surface), Federal Ministry of Education and Research (BMBF: ZIK/3DNano-Device), and Volkswagen Foundation in Germany.

**Supporting Information Available:** Large-area SEM images of a perfect UTAM and nanoparticle array with periods of 100 nm; comparison of SEM images of UTAMs and nanoparticle arrays with periods of 400 nm prepared by using PMMA as supporting layer and by our new technique. This material is available free of charge via the Internet at <http://pubs.acs.org>.

## REFERENCES AND NOTES

- Lee, S. H.; Cho, B.; Yoon, S.; Jeong, H.; Jon, S.; Jung, G. Y.; Cho, B. K.; Lee, T.; Kim, W. B. Printing of Sub-100-nm Metal Nanodot Arrays by Carbon Nanopost Stamps. *ACS Nano* **2011**, *5*, 5543–5551.
- Su, B.; Wang, S. T.; Ma, J.; Song, Y. L.; Jiang, L. “Clinging-Microdroplet” Patterning upon High-Adhesion, Pillar-Structured Silicon Substrates. *Adv. Funct. Mater.* **2011**, *21*, 3297–3307.
- Robinson, A. P.; Burnell, G.; Hu, M. Z.; MacManus-Driscoll, J. L. Controlled, Perfect Ordering in Ultrathin Anodic Aluminum Oxide Templates on Silicon. *Appl. Phys. Lett.* **2007**, *91*, 143123.
- Masuda, H.; Yanagishita, T.; Yasui, K.; Nishio, K.; Yagi, I.; Rao, T. N.; Fujishima, A. Synthesis of Well-Aligned Diamond Nanocylinders. *Adv. Mater.* **2001**, *13*, 247–249.
- Gates, B. D.; Xu, Q. B.; Stewart, M.; Ryan, D.; Willson, C. G.; Whitesides, G. M. New Approaches to Nanofabrication: Molding, Printing, and Other Techniques. *Chem. Rev.* **2005**, *105*, 1171–1196.
- Kramer, S.; Fuerer, R. R.; Gorman, C. B. Scanning Probe Lithography Using Self-Assembled Monolayers. *Chem. Rev.* **2003**, *103*, 4367–4418.
- Lei, Y.; Yang, S.; Wu, M.; Wilde, G. Surface Patterning Using Templates: Concept, Properties and Device Applications. *Chem. Soc. Rev.* **2011**, *40*, 1247–1258.
- Lei, Y.; Cai, W.; Wilde, G. Highly Ordered Nanostructures with Tunable Size, Shape and Properties: A New Way to Surface Nano-Patterning Using Ultra-Thin Alumina Masks. *Prog. Mater. Sci.* **2007**, *52*, 465–539.
- Rycenga, M.; Cobley, C. M.; Zeng, J.; Li, W.; Moran, C. H.; Zhang, Q.; Qin, D.; Xia, Y. Controlling the Synthesis and Assembly of Silver Nanostructures for Plasmonic Applications. *Chem. Rev.* **2011**, *111*, 3669–3712.
- Timmermans, M. Y.; Grigoras, K.; Nasibulin, A. G.; Hurskainen, V.; Franssila, S.; Ermolov, V.; Kauppinen, E. I. Lithography-Free Fabrication of Carbon Nanotube Network Transistors. *Nanotechnology* **2011**, *22*, 065303.
- Kustandi, T. S.; Loh, W. W.; Gao, H.; Low, H. Y. Wafer-Scale Near-Perfect Ordered Porous Alumina on Substrates by Step and Flash Imprint Lithography. *ACS Nano* **2010**, *4*, 2561–2568.
- Masuda, H.; Fukuda, K. Ordered Metal Nanohole Arrays Made by a 2-Step Replication of Honeycomb Structures of Anodic Alumina. *Science* **1995**, *268*, 1466–1468.
- Warkiani, M. E.; Bhagat, A. A. S.; Khoo, B. L.; Han, J.; Lim, C. T.; Gong, H. Q.; Fane, A. G. Isoporous Micro/Nanoengineered Membranes. *ACS Nano* **2013**, *7*, 1882–1904.
- Chong, Y. T.; Goerlitz, D.; Martens, S.; Yau, M. Y. E.; Allende, S.; Bachmann, J.; Nielsch, K. Multilayered Core/Shell Nanowires Displaying Two Distinct Magnetic Switching Events. *Adv. Mater.* **2010**, *22*, 2435–2439.
- Masuda, H.; Yamada, H.; Satoh, M.; Asoh, H.; Nakao, M.; Tamamura, T. Highly Ordered Nanochannel-Array Architecture in Anodic Alumina. *Appl. Phys. Lett.* **1997**, *71*, 2770–2772.
- Masuda, H.; Asoh, H.; Watanabe, M.; Nishio, K.; Nakao, M.; Tamamura, T. Square and Triangular Nanohole Array Architectures in Anodic Alumina. *Adv. Mater.* **2001**, *13*, 189–192.
- Masuda, H.; Abe, A.; Nakao, M.; Yokoo, A.; Tamamura, T.; Nishio, K. Ordered Mosaic Nanocomposites in Anodic Porous Alumina. *Adv. Mater.* **2003**, *15*, 161–164.
- Lee, W.; Ji, R.; Ross, C. A.; Gosele, U.; Nielsch, K. Wafer-Scale Ni Imprint Stamps for Porous Alumina Membranes Based on Interference Lithography. *Small* **2006**, *2*, 978–982.
- Lee, W.; Schwirn, K.; Steinhart, M.; Pippel, E.; Scholz, R.; Gosele, U. Structural Engineering of Nanoporous Anodic Aluminium Oxide by Pulse Anodization of Aluminium. *Nat. Nanotechnol.* **2008**, *3*, 234–239.
- Lee, W.; Han, H.; Lotnyk, A.; Schubert, M. A.; Senz, S.; Alexe, M.; Hesse, D.; Baik, S.; Gosele, U. Individually Addressable Epitaxial Ferroelectric Nanocapacitor Arrays with Near Tb Inch<sup>-2</sup> Density. *Nat. Nanotechnol.* **2008**, *3*, 402–407.
- Lee, W.; Ji, R.; Gosele, U.; Nielsch, K. Fast Fabrication of Long-Range Ordered Porous Alumina Membranes by Hard Anodization. *Nat. Mater.* **2006**, *5*, 741–747.
- Chou, S. Y.; Krauss, P. R.; Renstrom, P. J. Imprint Lithography with 25-Nanometer Resolution. *Science* **1996**, *272*, 85–87.
- Chik, H.; Xu, J. M. Nanometric Superlattices: Non-Lithographic Fabrication, Materials, and Prospects. *Mater. Sci. Eng. R* **2004**, *43*, 103–138.
- Lei, Y.; Chim, W. K. Highly Ordered Arrays of Metal/Semiconductor Core-Shell Nanoparticles with Tunable Nanostructures and Photoluminescence. *J. Am. Chem. Soc.* **2005**, *127*, 1487–1492.
- Wu, M.; Wen, L.; Lei, Y.; Ostendorp, S.; Chen, K.; Wilde, G. Ultrathin Alumina Membranes for Surface Nanopatterning in Fabricating Quantum-Sized Nanodots. *Small* **2010**, *6*, 695–699.
- Lei, Y.; Chim, W. K. Shape and Size Control of Regularly Arrayed Nanodots Fabricated Using Ultrathin Alumina Masks. *Chem. Mater.* **2005**, *17*, 580–585.
- Linic, S.; Christopher, P.; Ingram, D. Plasmonic-Metal Nanostructures for Efficient Conversion of Solar to Chemical Energy. *Nat. Mater.* **2011**, *10*, 911–921.

28. Xia, Y.; Xiong, Y.; Lim, B.; Skrabalak, S. E. Shape-Controlled Synthesis of Metal Nanocrystals: Simple Chemistry Meets Complex Physics? *Angew. Chem., Int. Ed.* **2009**, *48*, 60–103.
29. Chen, B.; Lu, K.; Tian, Z. Understanding Focused Ion Beam Guided Anodic Alumina Nanopore Development. *Electrochim. Acta* **2011**, *56*, 9802–9807.
30. Marimuthu, A.; Zhang, J. W.; Linic, S. Tuning Selectivity in Propylene Epoxidation by Plasmon Mediated Photo-Switching of Cu Oxidation State. *Science* **2013**, *339*, 1590–1593.
31. Liang, H.; Rossouw, D.; Zhao, H.; Cushing, S. K.; Shi, H.; Korinek, A.; Xu, H.; Rosei, F.; Wang, W.; Wu, N.; et al. Asymmetric Silver “Nanocarrot” Structures: Solution Synthesis and Their Asymmetric Plasmonic Resonances. *J. Am. Chem. Soc.* **2013**, *135*, 9616–9619.
32. Zhang, Q.; Li, W.; Moran, C.; Zeng, J.; Chen, J.; Wen, L.-P.; Xia, Y. Seed-Mediated Synthesis of Ag Nanocubes with Controllable Edge Lengths in the Range of 30–200 nm and Comparison of Their Optical Properties. *J. Am. Chem. Soc.* **2010**, *132*, 11372–11378.
33. Becker, J.; Zins, I.; Jakab, A.; Khalavka, Y.; Schubert, O.; Soennichsen, C. Plasmonic Focusing Reduces Ensemble Linewidth of Silver-Coated Gold Nanorods. *Nano Lett.* **2008**, *8*, 1719–1723.
34. Boisselier, E.; Astruc, D. Gold Nanoparticles in Nanomedicine: Preparations, Imaging, Diagnostics, Therapies and Toxicity. *Chem. Soc. Rev.* **2009**, *38*, 1759–1782.
35. Murphy, C. J.; Gole, A. M.; Hunyadi, S. E.; Stone, J. W.; Sisco, P. N.; Alkilany, A.; Kinard, B. E.; Hankins, P. Chemical Sensing and Imaging with Metallic Nanorods. *Chem. Commun.* **2008**, 544–557.
36. Dumond, J. J.; Low, H. Y. Recent Developments and Design Challenges in Continuous Roller Micro- and Nanoimprinting. *J. Vac. Sci. Technol. B* **2012**, *30*, 010801.